Journal of ELECTRONIC MATERIALS, Vol. 49, No. 5, 2020
https://doi.org/10.1007/s11664-020-08017-w

Electronic Transport and Non-linear Optical Properties of Hexathiopentacene (HTP) Nanorings: A DFT Study

İSKENDER MUZ[1] and MUSTAFA KURBAN[2,3]

1.—Department of Mathematics and Science Education, Nevşehir Hacı Bektaş Veli University, 50300 Nevşehir, Turkey. 2.—Department of Electronics and Automation, Kırşehir Ahi Evran University, 40100 Kırşehir, Turkey. 3.—e-mail: mkurbanphys@gmail.com

The electronic structure and structural and optoelectronic properties of hexathiopentacene (HTP) nanorings have been carried out by density functional theory (DFT) and time-dependent DFT (TD-DFT). Herein, the binding energy per atom, ionization potential, electron affinity, chemical hardness, highest occupied molecular orbital (HOMO)–lowest unoccupied molecular orbital (LUMO) gap, refractive index, charge distributions, absorbance spectra and non-linear optical properties have been measured. The calculations on these nanorings show that the HOMO–LUMO gaps range from 1.87 eV to 1.28 eV, which corresponds to the bandgap of known photovoltaic semiconductors, while the absorbance spectrum increases from 674 nm (1.84 eV) to 874 nm (1.42 eV), which indicates that the HTP nanorings absorb more light as the nanoring size is increased. From the binding energy, the stability of the HTP nanorings is higher than that of the HTP structure. Our results show that an increase in the size may play a significant role in improving the design of optoelectronic devices based upon these HTP nanorings.

Key words: HTP nanorings, electronic structure, bandgap, TD-DFT

INTRODUCTION

Recently, the design of organic semiconductor devices has drawn much attention in many applications such as photovoltaics,[1–5] light-emitting diodes,[6] photodetectors,[7] chemical, vapor and gas sensors.[8–12] Especially, organic semiconductors at the nanolevel are the most popular use for photovoltaic devices because of their unique electronic features. Therefore, it is highly significant to learn the role of the electronic structure of nanoscale organic molecules since that would have a tremendous impact on future electronic technologies.[13,14] While the linear chains and the 1D structures at the nano level have risen to the occasion in organic electronics,[15,16] the cyclic chains are of specific interest due to their excellent structural properties. Herein, much effort has been dedicated to building new nanotube components obtained from molecular structures because of their tunable photophysical features, supramolecular abilities[17,18] and their distinctive physical features thanks to changes in molecular size, shape, and crystallinity.[19–23] Thus, much effort for several decades has been focused on the synthesis of diverse nanorings.[17,22,24–29] In the first synthesized chiral nanoring experiment, all possible chiral structures of nanorings can be created by inserting various acenes with appropriate linkages.[27] Thus, advances in the design of nanorings have shown that it is possible to adjust the physical properties of organic molecules at the nanolevel to provide technological requirements for new devices with high efficiency. Moreover, it gives the possibility to find the best performing molecular semiconductors with very specific properties.

Acenes are a class of organic compounds made up of linear benzene rings (see Fig. 1). In this family, the order of increasing number of benzene rings is

(Received November 15, 2019; accepted February 12, 2020; published online February 21, 2020)

naphthalene, anthracene, tetracene, pentacene, and so on. In the literature, experimental investigations of the acene rings have been conducted in several studies. For example, the 2,6-naphthylene moiety, which is a derivation of naphthalene (n = 2), can easily rotate at ambient temperature.[30] In addition, cyclo-2,8-anthanthrylene (n = 3) has been synthesized in a few studies.[31,32] Recently, complex formation of different forms of an anthracene (n = 3) cyclic ring was synthesized by Toyota's group.[33] The properties of pentacene (n = 5) have recently attracted intensive interest. The hexathiopentacene (HTP) is one of the derivations of pentacene (n = 5) used as a p-type component in organic p–n-type heterostructures, which was widely used in a variety of solar cell applications.[34] In this context, the cyclic HTP nanorings have been designed to provide an insight to experimentalists on the nanorings because it is highly possible to synthesize the HTP nanorings for the reasons mentioned above.

To our knowledge, there is no information available about the electronic structure and structural and optical properties of the HTP nanorings. According to this viewpoint, we investigated the binding energy per atom, ionization potential, electron affinity, chemical hardness, HOMO–LUMO energy gap, refractive index, charge distributions. Non-linear optical (NLO) properties of the HTP nanorings have been researched using polarizability and hyperpolarizability.

COMPUTATIONAL DETAILS

The number of atoms in the HTP nanorings ranges from 72 (492 electrons) to 252 atoms (1722 electrons). Thus, we used the DFTB + code[35] with the hyb-0-2[36,37] set of Slater-Koster parameters to obtain the optimized geometry. This provides a reduction in computational time. In addition, our benchmarks show that the density-functional tight-binding (DFTB) optimization is more compatible with experimental data than that of density functional theory (DFT). In order to get more accurate energies, the single-point calculations are performed using DFT with B3LYP/6-311G(d,p) level.[38,39] In addition, the time-dependent (TD)-DFT calculations depending on the CAM-B3LYP functional[40] with 6-311G(d,p) basis set are used for estimating absorption spectra because B3LYP underestimates excited state energies.[41,42] Gaussian 09 software package was used in the calculations.[43]

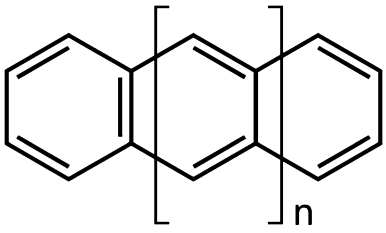

Fig. 1. The picture of acenes.

RESULTS AND DISCUSSION

Structure, Energy, Binding Energy, Stability

Figure 2 shows optimized geometries of HTP nanorings for N = 2 and 4. The corresponding total energies per atom of HTP nanorings are also listed in Table I. It is clear that there is an increase in total energy per atom, thus the HTP molecule is more reactive than HTP nanorings. Also, the HTP molecule has D_{2h} symmetry; however, after N = 2, it converts to C_{3h} for N = 3, C_{4h} for N = 4, C_{5h} for N = 5, C_{6h} for N = 6, C_{7h} for N = 7. The stability of the optimized structures was also calculated by binding energy per atom (E_b). E_b is a measure of its relative stability and it can be calculated as follows:

$$E_b(C_iS_jH_k) = \left[i \times E(C) + j \times E(S) + k \times E(H) - E(C_iS_jH_k)\right] / (i + j + k) \quad (1)$$

where $E(C)$, $E(S)$ and $E(H)$ are the energies of C, S and H atoms. $E(C_iS_jH_k)$ is also the total energy of the HTP structure. i, j and k are the number of atoms. The calculated binding energies per atom for the HTP nanorings are tabulated in Table I and shown in Fig. 3. The E_b value of HTP (1-HTP) is found to be 6.68 eV. The E_b of the HTP nanorings is strongly dependent on the number of the incorporated HTP. That is, an increase in the number of HTP nanorings causes an increase in the E_b which is the result of the stronger C–C double bonds

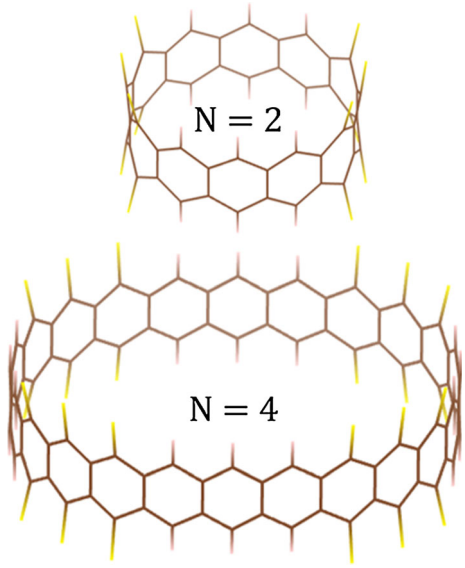

Fig. 2. Optimized geometries of HTP rings for N = 2 and 4 (Color figure online).

Table I. Structural properties and energies for HTP nanorings computed by B3LYP/6-311G(*d,p*) level

Structures	E_T	Symmetry	State	E_b
1-HTP	− 89.795716	D_{2h}	^1A	6.688
2-HTP	− 91.877937	D_{2h}	^1A	6.980
3-HTP	− 91.879075	C_{3h}	^1A	7.011
4-HTP	− 91.879429	C_{4h}	^1A	7.020
5-HTP	− 91.879580	C_{5h}	^1A	7.025
6-HTP	− 91.879654	C_{6h}	^1A	7.027
7-HTP	− 91.879696	C_{7h}	^1A	7.028

Total energy/per-atom (E_T, in a.u.) and binding energy (E_b, in eV.

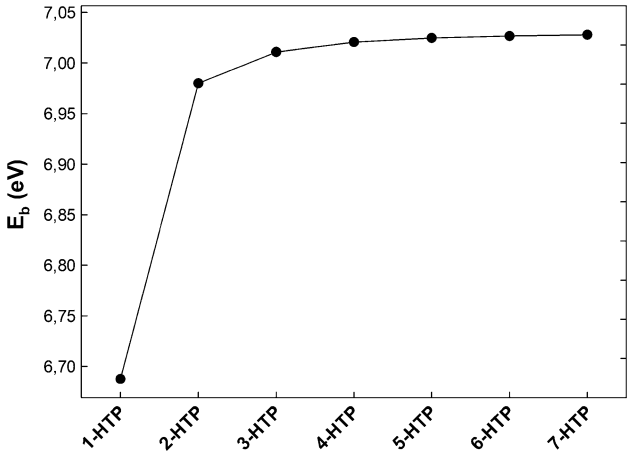

Fig. 3. Binding energy per atom (Eb) for HTP nanorings computed from B3LYP/6-311G(d,p) level of theory (Color figure online).

versus C–S bond. Thus, the E_b rapidly increases from 6.68 eV to 7.02 eV with increasing number of the HTP nanorings up to 4-HTP. Then, it is less pronounced and approximately stabilizes at about 7.03 eV (see Table I). This shows that the stability increases with an increase in the number of the HTP nanorings.

Bandgap, Ionization Potential and Electron Affinity

To investigate the electronic properties, the highest occupied molecular orbital (HOMO)–lowest unoccupied molecular orbital (LUMO), energy gap (E_g), vertical ionization potential (VIP) and vertical electron affinity (VEA) for the HTP nanorings were considered.

The bandgap is a useful property to probe the chemical activity of structure. The bandgap and HOMO–LUMO energy gap for the HTP nanorings are depicted in Fig. 4 and tabulated in Table II. For 1-HTP, the E_g value is 1.87 eV and then sharply decreases to 1.31 eV when it comes to 2-HTP. After

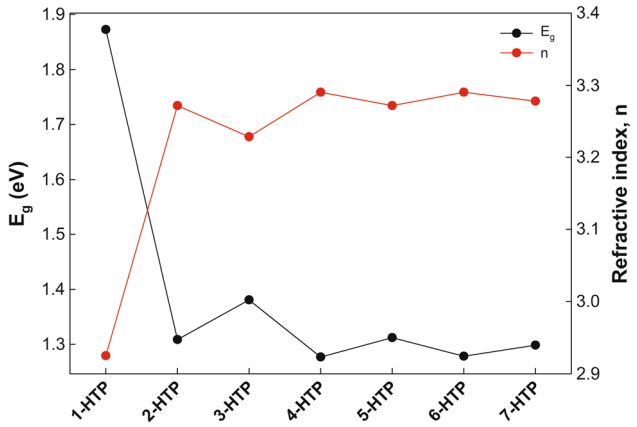

Fig. 4. HOMO-LUMO energy gap (Eg) and refractive index (n) for HTP nanorings computed from B3LYP/6-311G(d,p) level of theory (Color figure online).

that, it exhibits pronounced oscillating behavior with increasing number of HTPs. The calculated E_g value (1.87 eV) for 1-HTP is compatible with the experimental[44] value of 1.95–2.05 eV. In addition, E_g decreases to the lowest value of 1.28 eV for 4-HTP and 6-HTP. A lower gap means a smaller resistance against electronic excitation as well as a higher chemical reactivity. Therefore, the chemical reactivity of 4-HTP and 6-HTP is higher than their neighboring HTP nanorings. The bandgap is directly associated with electronic conductivity. Since the structures with lower bandgap show better conductance than the higher bandgap, 4-HTP and 6-HTP structures have the highest electronic conductivity. Depending on the number of the HTP nanorings, the bandgap, and thus the conductivity, is significantly changed. It is interesting to note that the bandgap of the even-membered HTP nanorings (2-, 4 and 6-HTP) is almost the same with the exception of some small oscillations, whereas it *decreases for* the odd-membered HTP nanorings (3-, 5 and 7-HTP). The bandgap oscillation is mostly due to the changes in the valance band maximum level, as shown in Table II. However, the conduction band minimum changes little for beyond 2-HTP, giving rise to the E_g oscillation, which is a direct consequence of the quantum confinement of the electrons. This behavior is also based on an increase in the number of atoms of the HTP nanorings, and it has also been observed in many carbon-based nanomaterials.[45,46] HOMO and LUMO concepts are associated with electron donating or electron withdrawing, and they play an important role in finding the reactivity of various materials with metal surface. A high HOMO shows a high tendency to donate electrons to appropriate acceptor material with low empty molecular orbital energy, whereas the high value of LUMO shows a low tendency to accept electrons from other materials. The HOMO value for 1-HTP is − 5.63 eV wide, i.e., about 0.23 eV greater than 7-HTP nanoring with 252

Table II. Electronic properties (in eV) for HTP nanorings at B3LYP/6-311G(*d*,*p*) level

	1-HTP	2-HTP	3-HTP	4-HTP	5-HTP	6-HTP	7-HTP
E_{HOMO}	− 5.63	− 5.26	− 5.41	− 5.34	− 5.40	− 5.38	− 5.40
E_{LUMO}	− 3.75	− 3.95	− 4.03	− 4.07	− 4.09	− 4.10	− 4.11
E_{gap}	1.87	1.31	1.38	1.28	1.31	1.28	1.30
VIP	6.83	6.16	6.14	5.94	5.93	5.83	5.83
VEA	2.56	3.04	3.31	3.47	3.57	3.64	3.70

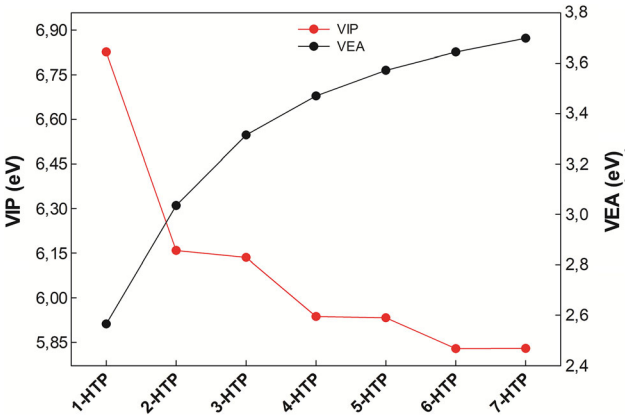

Fig. 5. Vertical ionization potentials (VIP) and vertical electron affinities (VEA) for HTP nanorings computed from B3LYP/6-311G(d,p) level of theory (Color figure online).

atoms. The 2-HTP nanoring with 72 atoms has the lowest HOMO value (− 5.26 eV), and thus it is less reactive due to the smallest HOMO value, while it is more stable than the other HTP nanorings (see Table II). On the other hand, the LUMO energy levels of the 1-HTP structure decrease from − 3.75 eV to − 4.11 eV, accordingly. From the obtained results, one can conclude that the 1-HTP structure is the most desirable structure in terms of accepting electrons, but the 7-HTP nanoring has the lowest tendency to donate electrons.

The ionization energy is the minimum energy necessary to remove an electron from a structure. VIP is defined as the energy difference between the optimized ground state of the cation and neutral. VIP is given by the following formula:

$$\mathrm{VIP} = E^{+} - E^{0} \tag{2}$$

where E^{+} and E^{0} are the ground state energy of the cation at the geometry of neutral and the ground state energy of neutral, respectively. Electron affinity is the energy released upon attachment of an electron to structure. VEA is defined as the energy difference between the optimized ground state of the anionic and neutral. VEA is given by the following formula:

$$\mathrm{VEA} = E^{0} - E^{-} \tag{3}$$

where E^{-} is the ground state energy of the anion at the optimized geometry of neutral. The data and the VIP and VEA plots are given in Fig. 5 and Table II. The VIP value decreases from 6.83 eV to 5.83 eV up to the 6-HTP nanoring, and then it remains constant at 5.83 eV for the 7-HTP nanoring. Based on an increase in the number of HTP nanorings, the VIP shows a decreasing trend, whereas the VEA shows an increasing trend. Figure 5 shows that the VEA value smoothly increases from 2.56 eV to 3.70 eV while the VIP value decreases from 6.83 eV to 5.83 eV for 1-HTP and 7-HTP, respectively,

The refractive index (n) values of the HTP nanorings can be found using the Ravindra relation,[47] which shows a linear relation between the n and E_g as follows:

$$n = 4.084 - 0.62E_g \tag{4}$$

The calculations show that n values are in the order: 1-HTP structure (2.924) < the HTP nanorings (from 3.228 to 3.290) due to a decrease in the bandgap, and its$n$ value inherently increases.

Global Reactivity Descriptors

It is well known that the chemical potential, chemical hardness and electrophilicity indexes are important fundamental quantities to explain reactivity and the molecular properties. For the HTP nanorings, therefore, the analysis of these global reactivity indices was considered in this study. The global reactivity descriptors can be described via using VIP and VEA energies of structure.

The chemical potential (μ) is defined as a measure of the escaping tendency of an electron for the ground state of a structure.[48] Chemical hardness (η) is also defined as the resistance of the chemical potential (resistance to charge transfer) to a change in the number of electrons.[49,50] The chemical potential and chemical hardness are given as following formula:

$$\mu = -(\mathrm{IP} + \mathrm{EA})/2 \tag{5}$$

$$\eta = (\mathrm{IP} - \mathrm{EA})/2 \tag{6}$$

Here, IP is ionization energy and EA is electron affinity. According to the principle of maximum

Table III. Reactivity properties (in eV) for HTP nanorings at B3LYP/6–311G(*d*,*p*) level

	1-HTP	2-HTP	3-HTP	4-HTP	5-HTP	6-HTP	7-HTP
η	2.13	1.56	1.41	1.23	1.18	1.09	1.07
μ	− 4.70	− 4.60	− 4.73	− 4.70	− 4.75	− 4.74	− 4.76
ω	5.17	6.77	7.92	8.97	9.57	10.27	10.65
ω^-	7.79	9.26	10.46	11.48	12.09	12.77	13.17
ω^+	3.09	4.66	5.73	6.77	7.34	8.04	8.40
ΔN_{max}	2.20	2.94	3.35	3.81	4.03	4.34	4.47

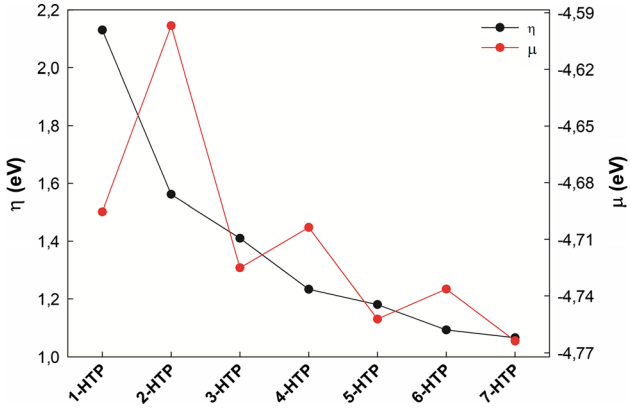

Fig. 6. Chemical hardness (η) and chemical potential (μ) for HTP nanorings computed from B3LYP/6-311G(d,p) level of theory (Color figure online).

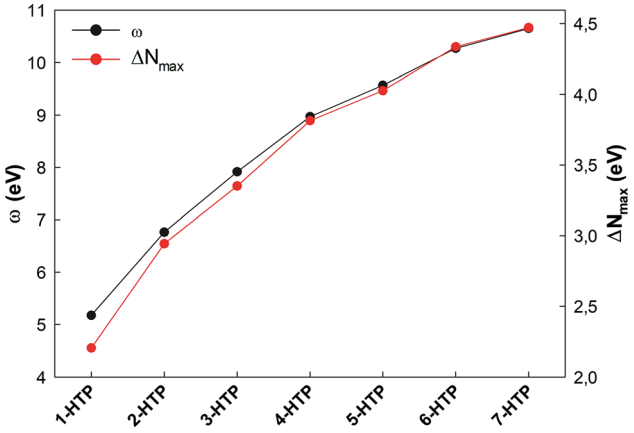

Fig. 7. Electrophilicity index (ω) and maximum amount of electronic charge index (ΔN_{max}) for HTP nanorings computed from B3LYP/6-311G(d,p) level of theory (Color figure online).

hardness (PMH),[51] a hard structure corresponds to a large energy gap. PMH can be readily understood from Eqs 4 and 5. A larger η value in the 1-HTP structure corresponds to a larger IP and a smaller EA, which implies that 1-HTP has more energy to accept an electron, that is, a lower tendency to give an electron and thus it is more stable than HTP nanorings. The values and the graphs of μ and η are presented in Table III and in Fig. 6. As is obvious from Table III, η remarkably decreases from 2.13 eV to 1.07 eV with an increase in the size of HTP nanoring. This indicates that the HTP structure has become chemically smoother. The μ is a key indicator of charge transfer during a chemical reaction and also electron pulling power, which is an important determinant of electronegativity (χ). From the results, the μ gradually decreases and shows oscillating behavior from 2-HTP to 7-HTP nanorings.

The electrophilicity index, ω is defined as a measure of the stabilization in energy when the structure acquires an electron acceptor from the environment.[52] In other words, it is a measure of the electrophilic power of system when two structures react with each other. It is given as the following formula:

$$\omega = \mu^2/2\eta \tag{7}$$

In addition, the electron donating (ω^-) and electron accepting (ω^+) powers have been given as

$$\omega^- = (3 \times \mathrm{IP} + \mathrm{EA})^2/16(\mathrm{IP} - \mathrm{EA}) \tag{8}$$

$$\omega^+ = (\mathrm{IP} + 3 \times \mathrm{EA})^2/16(\mathrm{IP} - \mathrm{EA}) \tag{9}$$

A larger ω^+ value in the structure corresponds to a better electron acceptor, whereas a smaller ω^- value implies that it is a better electron donor.[53] The values and the graphs of the electrophilicity indexes are tabulated in Table III and depicted in Fig. 7. As size of the HTP nanorings increases, ω, ω^- and ω^+ are increased significantly from 5.17 eV to 10.65 eV, from 7.79 eV to 13.17 eV and from 3.09 eV to 8.40 eV, respectively (Table III and Fig. 7). Since a higher electrophilicity index corresponds to more electrophilicity, 1-HTP structure has less electrophilicity than the HTP nanorings, but 7-HTP nanoring has the most electrophilicity.

The most accepted electron charge can be calculated from the maximum amount of electronic charge index (ΔN_{max}). It is given as the following formula:

$$\Delta N_{max} = -\mu/\eta \tag{10}$$

A positive ΔN_{max} demonstrates that charge flows to the system. Here, the system acts as an electron acceptor, whereas a negative ΔN_{max} indicates that

the system tends to donate its electrons. The maximum amount of electronic charge index has remarkably increased from 2.20 to 4.47 when it comes to an increase in the size of the HTP nanorings (see Table III and Fig. 7). This indicates that their affinity for accepting electrons has become effective with variation in size of the HTP nanorings.

Charge Distribution

The atomic charge distributions play an important part in the field of quantum chemical modeling to evaluate the electromagnetic properties of a structure, because they can affect polarizability, dipole moment, electronic and molecular properties.[54] In addition, the atomic charges for molecular structure give especially clear indications of the charge transfer, atomic charge displacements, and electrophilic and nucleophilic reactions. Herein, Mulliken charge distribution of the HTP nanorings is analyzed (see Fig. 8). In the HTP structure, Mulliken charge on sulfur (S) atoms has a positive charge due to the influence of surrounding electronegative carbon (C) atoms, but only a small portion has a negative charge. In addition, hydrogen (H) atoms carry also a positive charge. Mulliken charge on C atoms has a negative charge as a general trend, whereas a small portion has a positive charge. For HTP structure, charge transitions are generally from S and H to C atoms. The same trends are also observed with an increasing number of HTP nanorings. The average charges of S, H and C atoms are also presented in Fig. 8 and indicated with green, blue and red dashed lines, respectively. From the obtained results, S and H atoms are characteristically electropositive, whereas C is electronegative.

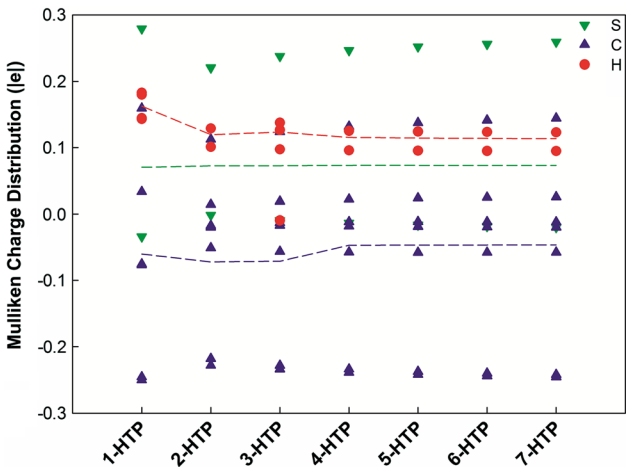

Fig. 8. Mulliken charge distributions for HTP nanorings computed from B3LYP/6-311G(d,p) level of theory (the dashed lines show the average value of the charges of S, C and H atoms) (Color figure online).

Non-linear Optical (NLO) Properties

Quantum chemical methods can be used to calculate various parameters such as polarizability and hyperpolarizability, which determines the efficiency of a structure to be used for potential nonlinear optical (NLO) material. NLO materials are commonly used in the fields of laser technology, optical devices, telecommunications and data storage.[55] To investigate the NLO characteristics, dipole moment (D_M), mean static polarizability (α_{tot}), anisotropic polarizability ($\Delta\alpha$) and first-order hyperpolarizability (β) were considered in this study. NLO properties for the HTP nanoring in terms of x, y, z components are calculated based on the same methodology as reported.[56–58]

A urea molecule is generally used in the calculation of NLO properties. In this study, the calculated NLO parameters are compared with those of urea and they are summarized in Table IV. The α_{tot} and $\Delta\alpha$ of 1-HTP structure are found to be 0.712×10^{-22} esu and 0.955×10^{-22} esu, respectively (see Table IV). In addition, the values of α_{tot} and $\Delta\alpha$ prominently increase with an increase in the number of HTP nanorings (from 2-HTP to 7-HTP). From Table IV, the value of first-order β for 1-HTP structure is found to be 15×10^{-30} esu which is approximately 94 times greater than that of urea (0.1591×10^{-30} esu) and much smaller than that of 7-HTP nanoring ($13{,}079 \times 10^{-30}$ esu). This indicates that the 1-HTP structure can be a candidate for NLO studies in the future. Considering the HTP nanorings, there is a considerable increase in the α_{tot} from 1.575×10^{-22} esu (2-HTP nanoring) to 10.386×10^{-22} esu (7-HTP nanoring). For 1-HTP structure, the higher value of β realized in the β_{xyz} direction point out more delocalization of the electron in the β_{xyz} direction. For the HTP nanorings, the values of β increase importantly with increasing size of HTPs. We should also mention that 1-HTP and the HTP nanorings show generally a good NLO activity. However, it is reported that for a structure to be considered a viable candidate it should first

Table IV. Non-linear optical properties, dipole moment (D_M, Debye), mean static polarizability (α_{tot}, (esu) $\times 10^{-22}$), anisotropic polarizability ($\Delta\alpha$, (esu) $\times 10^{-22}$) and first-order hyperpolarizability (β, (esu) $\times 10^{-22}$) for HTP nanorings computed from B3LYP/6-311G(*d*,*p*) level

	D_M	α_{tot}	$\Delta\alpha$	β
1-HTP	0.0001	0.712	0.955	15.0
2-HTP	0.0022	1.575	0.382	108.4
3-HTP	0.0032	2.967	1.575	912.7
4-HTP	0.0009	4.585	3.065	501.0
5-HTP	0.0017	6.421	4.872	1756.3
6-HTP	0.0010	8.363	6.834	1187.4
7-HTP	0.0066	10.386	8.914	13,079.0

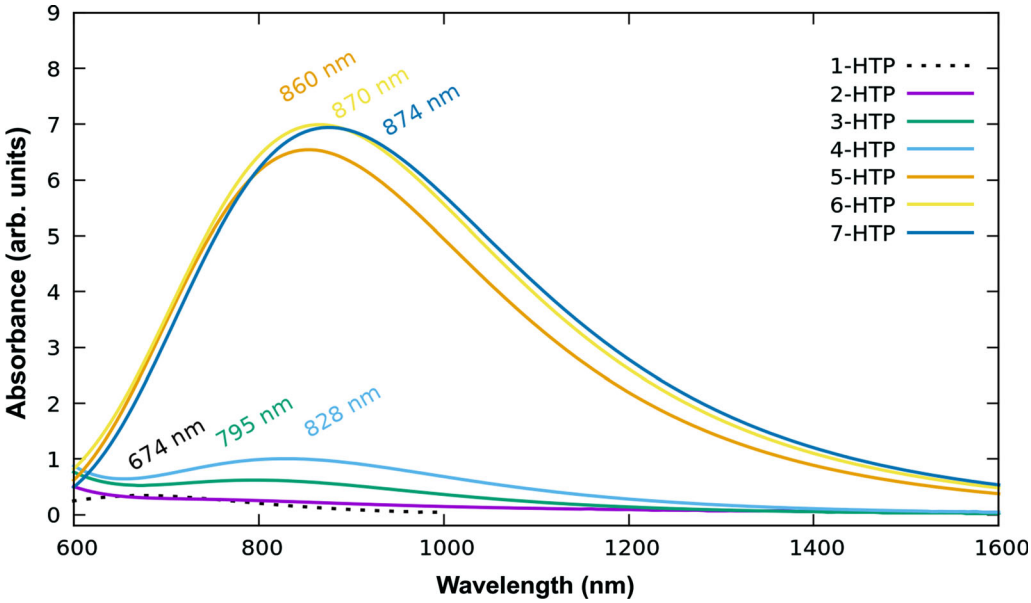

Fig. 9. UV-vis absorption spectra for HTP nanorings computed from CAM-B3LYP/6-311G(d,p) level of theory (Color figure online).

have a hyperpolarizability greater than approximately 500×10^{-30} esu.[59]

Optoelectronic Properties

The absorbance maxima of the HTP nanorings as a function of wavelength were shown in Fig. 9. The HTP single molecule exhibits the maximum peaks at 674 nm (1.84 eV). With the increase in the size of the HTP nanorings, there is a considerable increase up to 874 nm (1.42 eV) in the absorbance maxima. After 4-HTP nanoring, the peaks become wider and have higher magnitude from 5-HTP to the 7-HTP nanoring. From the results, the structures are shifted towards lower energy in going from HTP to the 7-HTP nanoring. It is interesting to note that the absorption magnitude difference from 674 nm (1-HTP) to 795 nm (2-HTP) is compatible with the bandgap (see Fig. 4), but the bandgap values of the HTP nanorings from 2-HTP to 7-HTP are relatively close to each other. As one may expect, the calculated bandgaps and absorption spectra strongly depend on the specific computational method. Here, we have used a B3LYP functional for bandgap calculations; however, the CAM-B3LYP functional has been used for absorption spectra because B3LYP underestimates excited state energies.[41,60,61] This may be a reason for the huge absorption magnitude difference between different structures. The second reason may be explained by the increasing number of atoms in the HTP nanorings, which has already been observed in C-based materials.[45]

CONCLUSIONS

The electronic structure, reactivity and non-linear optical properties of the HTP nanorings have been performed by DFT and TD-DFT methods. The bandgap of 1-HTP is found to be 1.87 eV and it is highly compatible with experimental results. According to the analysis of the energy, the bandgap shows a decreasing trend with an increase in the size of HTP nanorings. The refractive index of the HTP nanorings is greater than the 1-HTP structure. Moreover, the 1-HTP structure is more available to donate electrons than the HTP nanorings. Our results show that the chemical reactivity of HTP is lower than that of the HTP nanorings. The binding energy, which is also an indicator of stability, increases depending on a function of size. Therefore, the stability of the HTP nanorings is greater than that of the 1-HTP structure. Since 4-HTP and 6-HTP structures have the lowest bandgap, they are better in electronic conductivity than their neighbors. The absorption maxima become wider and have higher magnitude with an increase in the size of the HTP nanoring. It is important to note that studied HTP nanorings exhibit generally a good NLO activity.

ACKNOWLEDGMENTS

The numerical calculations were also partially performed at TUBITAK ULAKBIM, High Performance and Grid Computing Centre (TRUBA resources), Turkey.

REFERENCES

1. Q. Tu, Z. Yin, Y. Ma, S.-C. Chen, and Q. Zheng, *Dye Pigment* 149, 747 (2018).
2. C. Xie, P. You, Z. Liu, L. Li, and F. Yan, *Light. Appl.* 6, e17023 (2017).
3. W. Lee, J. Choi, and J.W. Jung, *Dye Pigment* 161, 283 (2019).
4. A. De Sio and C. Lienau, *Phys. Chem. Chem. Phys.* 19, 18813 (2017).

5. A.M. Nawar and M.M. Makhlouf, *J. Electron. Mater.* 48, 5771 (2019).
6. K. Xu, S. Hu, J. Hu, and X. Wang, *J. Electron. Mater.* 48, 838 (2019).
7. J.B. Wang, W.L. Li, B. Chu, C.S. Lee, Z.S. Su, G. Zhang, S.H. Wu, and F. Yan, *Org. Electron.* 12, 34 (2011).
8. F. Aziz, M.H. Sayyad, K. Sulaiman, B.H. Majlis, K.S. Karimov, Z. Ahmad, and G. Sugandi, *Meas. Sci. Technol.* 23, 014001 (2012).
9. M. Murugavelu, P.K.M. Imran, K.R. Sankaran, and S. Nagarajan, *Mater. Sci. Semicond. Process.* 16, 461 (2013).
10. R.N. Gillanders, I.D.W. Samuel, and G.A. Turnbull, *Sens. Actuat. B Chem.* 245, 334 (2017).
11. Y. Huang, R. Yuan, and S. Zhou, *J. Mater. Chem.* 22, 883 (2012).
12. M.E. Harb, S. Ebrahim, M. Soliman, and M. Shabana, *J. Electron. Mater.* 47, 353 (2018).
13. H. Jiang, X.-N. Hu, Y.-C. Zhao, and C. Zhang, *J. Electron. Mater.* 46, 1005 (2017).
14. B.M. Wong and A.M. Morales, *J. Phys. D Appl. Phys.* 42, 055151 (2009).
15. X. Zhou, T. Zifer, B.M. Wong, K.L. Krafcik, F. Leonard, and A.L. Vance, *Nano Lett.* 9, 1028 (2009).
16. B.M. Wong, F. Leonard, Q. Li, and G.T. Wang, *Nano Lett.* 11, 3074 (2011).
17. R. Jasti, J. Bhattacharjee, J.B. Neaton, and C.R. Bertozzi, *J. Am. Chem. Soc.* 130, 17646 (2008).
18. J. Xia, J.W. Bacon, and R. Jasti, *Chem. Sci.* 3, 3018 (2012).
19. D.J. Cram and J.M. Cram, *Acc. Chem. Res.* 4, 204 (1971).
20. U. Girreser, D. Giuffrida, F.H. Kohnke, J.P. Mathias, D. Philp, and J.F. Stoddart, *Pure Appl. Chem.* 65, 119 (1993).
21. L.T. Scott, *Angew. Chem. Int. Ed.* 42, 4133 (2003).
22. K. Tahara and Y. Tobe, *Chem. Rev.* 106, 5274 (2006).
23. T. Kawase and H. Kurata, *Chem. Rev.* 106, 5250 (2006).
24. R. Jasti and C.R. Bertozzi, *Chem. Phys. Lett.* 494, 1 (2010).
25. M. Fujitsuka, D.W. Cho, T. Iwamoto, S. Yamago, and T. Majima, *Phys. Chem. Chem. Phys.* 14, 14585 (2012).
26. M. Fujitsuka, C. Lu, T. Iwamoto, E. Kayahara, S. Yamago, and T. Majima, *J. Phys. Chem. A* 118, 4527 (2014).
27. H. Omachi, Y. Segawa, and K. Itami, *Org. Lett.* 13, 2480 (2011).
28. H. Takaba, H. Omachi, Y. Yamamoto, J. Bouffard, and K. Itami, *Angew. Chem. Int. Ed.* 48, 6112 (2009).
29. S. Yamago, Y. Watanabe, and T. Iwamoto, *Angew. Chem. Int. Ed.* 49, 757 (2010).
30. J.E. Mcmurry, G.J. Haley, J.R. Matz, J.C. Clardy, and J. Mitchell, *J. Am. Chem. Soc.* 108, 515 (1986).
31. V. Sgobba and D.M. Guldi, *Chem. Soc. Rev.* 38, 165 (2009).
32. S. Hitosugi, T. Yamasaki, and H. Isobe, *J. Am. Chem. Soc.* 134, 12442 (2012).
33. Y. Yamamoto, E. Tsurumaki, K. Wakamatsu, and S. Toyota, *Angew. Chemie Int. Ed.* 57, 8199 (2018).
34. P. Lutsyk and Y. Vertsimakha, *Mol. Cryst. Liq. Cryst.* 426, 265 (2005).
35. B. Aradi, B. Hourahine, and T. Frauenheim, *J. Phys. Chem. A* 111, 5678 (2007).
36. B. Szucs, Z. Hajnal, R. Scholz, S. Sanna, and T. Frauenheim, *Appl. Surf. Sci.* 234, 173 (2004).
37. B. Szucs, Z. Hajnal, T. Frauenheim, C. Gonzalez, J. Ortega, R. Perez, and F. Flores, *Appl. Surf. Sci.* 212, 861 (2003).
38. A.D. Becke, *J. Chem. Phys.* 98, 1372 (1993).
39. C. Lee, W. Yang, and R.G. Parr, *Phys. Rev. B* 37, 785 (1988).
40. T. Yanai, D.P. Tew, and N.C. Handy, *Chem. Phys. Lett.* 393, 51 (2004).
41. M. Kurban, B. Gündüz, and F. Göktaş, *Optik (Stuttg).* 182, 611 (2019).
42. I. Muz and M. Kurban, *J. Alloys Compd.* 802, 25 (2019).
43. M.J. Frisch, G.W. Trucks, H.B. Schlegel, G.E. Scuseria, M.A. Robb, J.R. Cheeseman, G. Scalmani, V. Barone, B. Mennucci, G.A. Petersson, H. Nakatsuji, M. Caricato, X. Li, H. P. Hratchian, A. F. Izmaylov, J. Bloino, G. Zheng, J.L. Sonnenberg, M. Hada, M. Ehara, K. Toyota, R. Fukuda, J. Hasegawa, M. Ishida, T. Nakajima, Y. Honda, O. Kitao, H. Nakai, T. Vreven, J.A. Montgomery, J.E. Peralta, F. Ogliaro, M. Bearpark, J.J. Heyd, E. Brothers, K.N. Kudin, V.N. Staroverov, R. Kobayashi, J. Normand, K. Raghavachari, A. Rendell, J. C. Burant, S.S. Iyengar, J. Tomasi, M. Cossi, N. Rega, J.M. Millam, M. Klene, J.E. Knox, J.B. Cross, V. Bakken, C. Adamo, J. Jaramillo, R. Gomperts, R.E. Stratmann, O. Yazyev, A.J. Austin, R. Cammi, C. Pomelli, J.W. Ochterski, R.L. Martin, K. Morokuma, V.G. Zakrzewski, G.A. Voth, P. Salvador, J.J. Dannenberg, S. Dapprich, A.D. Daniels, Farkas, J.B. Foresman, J.V Ortiz, J. Cioslowski, D.J. Fox, Gaussian Inc., Wallingford CT (2009).
44. Y. Vertsimakha and P. Lutsyk, *Mol. Cryst. Liq. Cryst.* 467, 107 (2007).
45. Y. Saleem, L.N. Baldo, A. Delgado, L. Szulakowska, and P. Hawrylak, *J. Phys. Condens. Mater.* 31, 305503 (2019).
46. A.D. Gueclue, P. Potasz, and P. Hawrylak, *Phys. Rev. B* 82, 1 (2010).
47. N.M. Ravindra, S. Auluck, and V.K. Srivastava, *Phys. Status Solidi B* 93, K155 (1979).
48. R.G. Parr and W.T. Yang, *J. Am. Chem. Soc.* 106, 4049 (1984).
49. R.G. Parr and R.G. Pearson, *J. Am. Chem. Soc.* 105, 7512 (1983).
50. R.G. Pearson, *J. Chem. Sci.* 117, 369 (2005).
51. R.G. Pearson, *Acc. Chem. Res.* 26, 250 (1993).
52. R.G. Parr, L. Von Szentpaly, and S.B. Liu, *J. Am. Chem. Soc.* 121, 1922 (1999).
53. J.L. Gazquez, A. Cedillo, and A. Vela, *J. Phys. Chem. A* 111, 1966 (2007).
54. M.V.S. Prasad, N.U. Sri, and V. Veeraiah, *Spectrochim. Acta Part A Mol. Biomol. Spectrosc.* 148, 163 (2015).
55. X. Zhang, M. Li, Z. Shi, and Z. Cui, *Mater. Lett.* 65, 1404 (2011).
56. D. Sajan, H. Joe, V.S. Jayakumar, and J. Zaleski, *J. Mol. Struct.* 785, 43 (2006).
57. Y.-X. Sun, Q.-L. Hao, Z.-X. Yu, W.-X. Wei, L.-D. Lu, and X. Wang, *Mol. Phys.* 107, 223 (2009).
58. N. Sundaraganesan, E. Kavitha, S. Sebastian, J.P. Cornard, and M. Martel, *Spectrochim. Acta Part A Mol. Biomol. Spectrosc.* 74, 788 (2009).
59. M.D.H. Bhuiyan, M. Ashraf, A. Teshome, G.J. Gainsford, A.J. Kay, I. Asselberghs, and K. Clays, *Dye Pigment* 89, 177 (2011).
60. M.E. Foster and B.M. Wong, *J. Chem. Theory Comput.* 8, 2682 (2012).
61. S.K. Dutta, S.K. Mehetor, and N. Pradhan, *J. Phys. Chem. Lett.* 6, 936 (2015).